Particle production in $\sqrt{s_{NN}} = 2.76$ TeV heavy ion collisions

Johann Rafelski[1] and Jean Letessier[1,2]
[1]*Department of Physics, University of Arizona, Tucson, Arizona 85721, USA*
[2]*LPTHE, Université Paris 6 et 7, Paris F-75005, France*
(Received 7 December 2010; published 23 May 2011)

We obtain within the statistical hadronization model (SHM) the hadron yields dh/dy in heavy ion reactions at $\sqrt{s_{NN}} = 2.76$ TeV. We discuss the dependence both on hadronization temperature T and on critical hadronization pressure P. We consider observables distinguishing the hadronization models and conditions.

DOI: 10.1103/PhysRevC.83.054909 PACS number(s): 12.38.Mh, 24.10.Pa, 25.75.−q

I. INTRODUCTION

According to the theory of strong interactions—quantum chromodynamics (QCD)—quarks and gluons are confined inside hadrons. Lattice computations demonstrate that the deconfined quark-gluon plasma (QGP) is present at high temperature [1]. To prove this QCD paradigm, heavy nuclei are crushed on each other, forming a small drop of thermalized, deconfined QGP matter. QGP hadronizes, and we seek to determine the physical properties of QGP considering this multihadron final state.

At the CERN Large Hadron Collider (LHC) energy $\sqrt{s_{NN}} = 2.76$ TeV, for near head-on (only 5% off center, i.e. 5% most central) Pb-Pb collisions, the pseudorapidity density of primary charged particles at midrapidity is $dh/d\eta = 1584 \pm 4 \pm 76$ syst., an increase of about a factor 2.2 over central Au-Au BNL Relativistic Heavy Ion Collider (RHIC) collisions at $\sqrt{s_{NN}} = 0.2$ TeV [2]. Following Ref. [3], where deformation of the spectra were studied in model cases, we interpret the measured $dh/d\eta$ to be equivalent to a central rapidity density $dh/dy \simeq 1800 \pm 100$.

This first LHC-ion total hadron multiplicity experimental result enables us to offer quantitative predictions for a variety of different particle multiplicities. The study of particle yields per unit of rapidity obtained after integration of transverse-momentum particle spectra eliminates the need to model the distortion of spectra introduced by explosive dynamics (see, e.g., Ref. [3]) of highly compressed matter created in high-energy collisions. Thus, total particle (rapidity) yields are good experimental observables. We note that for n independent particle yields, there are $n(n-1)/2$ particle ratios, and this tempts us to switch to ratios as an observable. However, $n(n-1)/2$ data points are originating in n independent measurements only, and each ratio has an experimental error considerably greater compared to an individual yield. Thus we choose to study yields both to avoid redundancy and to achieve the highest available precision.

The procedure outlined earlier [4] is applied to these first LHC experimental data within two versions of a statistical hadronization model (SHM), i.e., the chemical equilibrium model and the chemical nonequilibrium model. We will present absolute particle yields given that dh/dy is fixed. For the nonequilibrium model we (a) prescribe a hadronization pressure condition [5], discovered in comparative RHIC and CERN Super Proton Synchrotron (SPS) hadronization studies; and (b) prescribe strangeness yield per entropy derived from kinetic study of strangeness production in QGP [6].

II. SHM

The SHM [7–9] is widely used in describing hadron production in heavy ion collisions for different colliding systems and energies. Some view the SHM as a qualitative model, and as such one is tempted to seek simplicity in an effort to obtain an estimate of the yields for all hadrons with just a small number of parameters [10–12].

Improvements in experimental precision, along with physics motivation based in qualitative dynamics of the hadronization process, have stimulated refinements involving a greater parameter set, allowing us to control the dynamically established yield of different quark flavors, generally referred to as the chemical nonequilibrium SHM [8]. This is achieved by introducing statistical occupancy parameters $\gamma_i > 1$, $i = q, s, c$, where s is the strange and c the charm quark flavor. It can be assumed that up and down quark yields $q = u, d$ are equally equilibrated. We will not discuss the charm flavor here.

Moreover, we are interested in precise description of the bulk properties of the particle source, such as size, energy, and entropy content of the QGP fireball. This requires precise capability to extrapolate observed hadron yields to unobserved kinematic domains and unobserved particle types. This is the case for the chemical-nonequilibrium approach, as demonstrated by the smooth systematic behavior of physical observables as a function of collision conditions such as reaction energy [8] or collision centrality [13].

With increasing collision energy, the baryon content at central rapidity decreases rapidly. It is expected that there remains a small excess of matter over antimatter at central rapidity at the LHC [14]. In the SHM, this is governed by chemical parameters λ_q, λ_s (equivalent to μ_B, μ_S, the baryon and strangeness chemical potentials of matter). Note that since the number of strange and antistrange quarks balances overall and within the observed rapidity acceptance is known to balance to better than 3% at the RHIC, λ_s, and thus μ_S, is determined in order to satisfy this net strangeness conservation constraint.

Another constraint is also implemented: The total charge per baryon has to be $Q/B = 0.4$, since the stopping of

electrically charged matter (protons) within a rapidity interval is the same as that of all baryonic matter (protons and neutrons). This is achieved by a suitable (tiny) up-down quark asymmetry, a feature implemented in the SHARE suite of programs we are using [7].

In the usual SHM procedure, the particle yields are used to find best statistical parameters. The SHARE suite of programs was written in a more flexible way to allow also mixed-fit, i.e., a fit where a few particle yields can be combined with the given "measured" statistical parameters and/or physical properties to obtain the best fit of other statistical parameters. When we were developing SHARE, this feature was created since a parameter such as temperature could be measured using spectral shape and thus should be not fitted again in the yield description but should be used as an experimental input. To generalize, this feature was extended to all statistical parameters and fireball physical properties of the SHARE program, and we use this feature here to perform a fit of the mix of statistical parameters, physical properties, and particle yield.

III. IMPORTANCE OF UNDERSTANDING CHEMICAL (NON)EQUILIBRIUM

When chemical nonequilibrium is derived from the particle yields, generating the fit to data $\gamma_i \neq 1$, this suggests a dynamic picture of an explosively expanding and potentially equilibrated QGP, decaying rapidly into free-streaming hadrons. Without significant reequilibration, the (nearly) equilibrated QGP cannot produce a chemically equilibrated hadron yield. The high intrinsic QGP entropy content explains why equilibrated QGP turns into chemically overpopulated (oversaturated) hadron gas (HG) phase space. The fast breakup of QGP means that the emerging hadrons do not have an opportunity to reestablish chemical equilibrium in the HG phase.

The differentiation of chemical-equilibrium and -nonequilibrium SHMs will be one of the challenges we address in our present discussion about the SHM and interpretation of the hadron production. One could think that resolution of this matter requires a good fit of SHM parameters to the data. However, with the large errors on particle yields and lack of sensitivity to γ_q, this is not easy, and thus we present chemical-equilibrium and -nonequilibrium conditions in turn. For a prescribed dh/dy, we will show that many, but not all, particle yields vary little as a function of the hadronization condition assumed, making the resolution of this question difficult.

The light-quark phase-space occupancy parameter γ_q can be measured only by determining overall baryon to meson yield, and this cannot be done without prior measurement of the hadronization temperature T. When particle yield data are not available to measure both T and γ_q, one can fit only γ_s/γ_q to the data, which is then reported as γ_s accompanied by the tacit assumption $\gamma_q = 1$. Since γ_s (or γ_s/γ_q) controls the overall (relative) yield of strange quarks, one expects and finds in most environments $\gamma_s \neq 1$ (or $\gamma_s/\gamma_q \neq 1$) and a value that increases with system size, and often with energy.

We recognize considerable physics implications of understanding the value of γ_q, as this relates directly to the measurement of T, the (chemical freeze-out) temperature at which hadron yields are established. Upon formation, hadrons can interact while expanding; however, upon integration of the spectrum to obtain yields, there is no memory of this process and of the related kinetic freeze-out temperature. The chemical freeze-out temperature T is related to the phase-transformation condition $T_{\rm tr}$ of QGP to hadrons, studied within lattice QCD. In the hadron chemical-equilibrium context, which presumes that a slow transition occurs, it is the general assumption that $T \simeq T_{\rm tr}$. The chemical-nonequilibrium SHM implies rapid expansion and supercooled transformation, hence $T < T_{\rm tr}$, with estimated difference at 10–15 MeV [15]. One can argue that this effect has been observed.

For lower heavy ion reaction energies as compared to LHC energies, one can determine the baryochemical potential at hadronization. This then allows the comparison of the lattice QCD transformation condition $T_{\rm tr}$, $\mu_{B,\rm tr}$ [16,17], with the data fit in the chemical-equilibrium SHM [14,18] and the chemical-nonequilibrium SHM [8]. One finds that lattice results are flatter compared to the equilibrium SHM [19]; i.e., $T_{\rm tr}$ drops off slower with $\mu_{B,\rm tr}$. On the other hand, the nonequilibrium SHM parallels the lattice data 10–15 MeV below the transformation boundary as predicted. In our opinion, this favors, on theoretical grounds, the chemical-nonequilibrium approach.

IV. LHC PREDICTIONS ASSUMING CHEMICAL EQUILIBRIUM

Our procedure for the equilibrium SHM is as follows: in the chemical-equilibrium model (see Table I), we set $\gamma_q = 1$, $\gamma_s = 1$. All our results maintain a fixed ratio $Q/B = 0.4$. We fix as input value $\lambda_q = 1.0055$; λ_s follows from the constraint of strangeness balance. The choice of λ_q is arbitrary but realistic for the circumstance, and we opted to do this instead of taking $\lambda_q = \lambda_s = 1$ in order to establish how difficult the observation of baryon asymmetry at central rapidity could be. This results in $\mu_B \simeq 2.9 \pm 0.3$ MeV, $\mu_S \simeq 0.7 \pm 0.3$ MeV, respectively, at fixed hadronization temperature T chosen in Table I to be 159, 169, 179, and 189 MeV.

We choose to present a relatively wide range of hadronization temperature cases in order to show how various observables depend on T, and to allow comparison with other groups addressing this range of values [11,20,21]. For the same reason, we present an unusual number of digits, a precision needed to facilitate the reproducibility of our results. We further state, in Table I, the propagation of the error $\Delta\, dh/dy = 100$. We see, in Table I, the yield of charged hadrons dh/dy correlated to the source volume dV/dy. Volume varies strongly with temperature, since particle yields scale, for $T \gg m$, as VT^3. Actually, since the $T \gg m$ condition is not satisfied, the volume is changing more rapidly, so that $T^k dV/dy = \text{const}$, $k \simeq 7.2$.

Since the charged particle number is fixed $dh/dy \simeq 1800$, we also expect that the entropy of the bulk matter of the fireball (bulk) is fixed, and that is true; up to a small variation due to variation with T in relative yield of heavy hadrons, the entropy content is $dS/dy = 14\,800 \pm 400$. As temperature increases, the proportion of heavy-mass charged particles increases, and

TABLE I. Chemical-equilibrium particle yields at $\sqrt{s_{NN}} = 2.76$ TeV. Top section: input properties; middle section: properties of the fireball associated with central rapidity; bottom section: expected particle yields, and some select ratios. * signals an input value, and ** a result directly following from an input value (combined often with a constraint). All yields, except $\pi^0_{\rm WD}$, without weak decay feed to particle yields. Error in dV/dy corresponds to error in $dh/dy = 100$.

T^* (MeV)	159	169	179	189
γ_q^*	1	1	1	1
γ_s^*	1	1	1	1
λ_q^*	1.0055	1.0055	1.0055	1.0055
$10^3(\lambda_s - 1)^{**}$	2.06	1.45	0.89	0.39
$(Q/B)^*$	0.4000	0.4000	0.4000	0.4000
$(s - \bar{s})^*$	0.0000	0.0000	0.0000	0.0000
$(dh/dy)^*$	1800	1800	1800	1800
dV/dy (fm^3)	5285 ± 147	3452 ± 96	2286 ± 64	1538 ± 43
dS/dy	15 155	14 940	14 690	14 420
s/S	0.0245	0.0255	0.0263	0.0270
P (MeV/fm^3)	64.1	100	153	231
E/TS	0.859	0.86	0.87	0.87
P/E	0.164	0.158	0.153	0.150
E/V (GeV/fm^3)	0.392	0.632	0.997	1.54
π^-, π^+	839	830	821	813
K^-	141.3	140.8	139.0	136.8
K^+	142.1	141.6	140.1	137.8
p	53.6	63.1	72.0	79.8
$\bar{p}$	51.9	61.2	69.7	77.3
Λ	30.0	36.3	42.1	47.3
$\overline{\Lambda}$	29.2	35.4	41.1	46.2
Ξ^-	4.45	5.47	6.41	7.23
$\overline{\Xi}^+$	4.36	5.38	6.31	7.14
Ω^-	0.772	1.038	1.314	1.586
$(B - \overline{B})^{**}$	4.81	5.60	6.29	6.88
ρ	92.4	96.6	99.1	100.3
ϕ	19.0	20.5	21.4	21.9
$K^{0*}(892)$	42.6	45.3	46.9	47.6
$K^{0*}(892)/K^-$	0.301	0.322	0.337	0.348
$\phi/K^{0*}(892)$	0.446	0.452	0.456	0.460
π^0	942	933	925	916
η	110	111	111	110
η'	9.67	10.4	10.8	11.1
$\pi^0_{\rm WD}$	1251	1251	1249	1245

thus the pion yield and even the kaon yield slightly decrease with increasing T. Baryon yield is most sensitive to T: Ω doubles in yield in the temperature interval considered. Our choice of λ_q fixes for each hadronization temperature the per-rapidity net baryon yield also shown in Table I. We believe our choice is reasonable, and it shows that there is no need to distinguish particles from antiparticles.

Strangeness yield increases slightly with T; this increase is found in heavy-mass strange baryons, e.g., Λ, and this depletes slightly the yield of kaons. Overall the specific strangeness per entropy yield grows very slowly from $s/S = 0.0245$ to 0.027. Several ratios, such as $\phi/K^{0*}(892) \simeq 0.45$, where several effects compensate, are nearly constant.

We also show the post-weak-decay $\pi^0_{\rm WD}$ yield, which is relatively large and independent of hadronization T. The decay $\pi^0 \to \gamma\gamma$ generates a strong electromagnetic energy component.

V. LHC PREDICTION WITHIN NONEQUILIBRIUM SHM

Within the nonequilibrium hadronization approach, we need to further anchor the quark-pair abundance parameters γ_q and γ_s. In the absence of experimental data, we introduce as hadronization conditions the relative strangeness yield s/S and hadronization pressure P. We vary P (see Table II) just as we varied T, the hadronization condition in the chemical-equilibrium model. In the chemical-nonequilibrium SHM, two conditions suffice to narrow considerably the values of three SHM parameters (γ_q, γ_s, and T), but only if we insist that a third condition $E/TS > 1$ is qualitatively satisfied.

Strangeness yield is a natural hadronization condition of QGP. The QGP expected dynamic strangeness yield is considerably higher than the chemical-equilibrium yield (Table I). The greater strangeness content in QGP is, in fact,

TABLE II. Chemical-nonequilibrium particle yields, each column for different hadronization pressure. See caption of Table I for further details.

P^* (MeV/fm^3)	60.3	70.0	82.2	90.1
$(s/S)^*$	0.0367	0.0370	0.0370	0.0373
λ_q^*	1.0055	1.0055	1.0055	1.0055
$10^3(\lambda_s - 1)^{**}$	2.69	2.45	2.19	2.04
$(Q/B)^*$	0.400	0.400	0.4000	0.4000
$(s - \bar{s})^*$	0.0000	0.0000	0.0000	0.0000
$(dh/dy)^*$	1800	1800	1800	1800
T (MeV)	131.2	134.3± 0.1	137.7± 0.1	139.6± 0.1
γ_q	1.599 ± 0.001	1.600 ± 0.008	1.601 ± 0.009	1.599 ± 0.011
γ_s	2.913 ± 0.008	2.842 ± 0.030	2.745 ± 0.030	2.721 ± 0.016
dV/dy (fm^3)	5469 ± 542	4731 ± 136	4043 ± 119	3705 ± 168
dS/dy	13 924	13 879	13 794	13 797
E/TS	1.060	1.060	1.059	1.059
P/E	0.170	0.168	0.165	0.164
E/V (GeV/fm^3)	0.354	0.417	0.497	0.550
π^-, π^+	858	854	850	848
K^-	192.0	190.2	186.5	186.2
K^+	192.9	191.2	187.5	187.3
p	32.9	36.3	40.3	42.5
$\bar{p}$	31.8	35.2	39.0	41.2
Λ	28.9	31.8	34.8	36.9
$\overline{\Lambda}$	28.1	31.0	33.9	35.9
Ξ^-	6.92	7.56	8.12	8.60
$\overline{\Xi}^+$	6.77	7.40	7.96	8.43
Ω^-	1.56	1.73	1.89	2.03
$(B - \overline{B})^{**}$	3.640	3.973	4.328	4.539
ρ	56.1	58.8	61.7	63.2
ϕ	30.0	30.7	30.8	31.4
$K^{0*}(892)$	39.9	41.4	42.6	43.6
$K^{0*}(892)/K^-$	0.208	0.218	0.228	0.234
$\phi/K^{0*}(892)$	0.751	0.741	0.722	0.721
π^0	988	983	979	977
η	134	132	128	128
η'	10.4	10.7	10.8	11.0
$\pi^0_{\rm WD}$	1398	1396	1389	1391

the reason behind the interest in strangeness as a signature of QGP. $s\bar{s}$ pairs are produced predominantly in thermal gluon processes, and their yield can be obtained within the QCD perturbative approach. In a study that was refined to agree with the strangeness yield observed at the RHIC, we predicted the value $s/S \simeq 0.037$ for the LHC [6]. We use here this result, noting that higher s/S values are possible, depending on LHC-formed QGP dynamics.

The second condition arises from the observation that once the statistical parameters were fitted across diverse reaction conditions at the RHIC, the one constant outcome was that the hadronization pressure $P = 82$ MeV/fm^3 [5]. Choice of pressure as a natural QGP hadronization constraint is further rooted in the observation that the vacuum confinement phenomenon can be described within the qualitative MIT-bag model of hadrons introducing vacuum pressure as $B_{\rm MIT} = 58$ MeV/fm^3; while in a bag-motivated fit to hadron spectra, which allows additional flexibility in parameters, one finds $B_{\rm fit} = 112$ MeV/fm^3 [22]. Clearly, a range of values is possible theoretically, with the hadronization condition $P = 82$ MeV/fm^3 right in the middle of this domain. We will use this "critical-pressure" hadronization condition as our constraint, but also vary it such that $60 \leqslant P \leqslant 90$ MeV/fm^3 so that we can be sure that our prediction is not critically dependent on the empirical value. The pressure seen in the equilibrium model (Table I) has a range $64 \leqslant P \leqslant 230$ MeV/fm^3.

The third constraint is not imposed in its precise value, but we require that hadronization occur under the constraint $E/TS > 1$. In comparison, for the equilibrium case (Table I) we have $0.86 < E/TS < 0.87$, a relatively small variation. The importance of this quantity $E/TS > 1$ as a diagnostic tool for explosive QGP outflow and hadronization was discussed in Ref. [15]. In fact, we find that a reasonable and stable hadronization arises in chemical nonequilibrium within a narrow interval $1.059 < E/TS < 1.060$. Finally, the baryon

asymmetry is treated in the same way as in the chemical-equilibrium model, fixed $\lambda_q = 1.0055$, implies now $\mu_B \simeq 2.0 \pm 0.2$ MeV, $\mu_S \simeq 0.45 \pm 0.05$ MeV.

In Table II, the outcome of this procedure is presented. We state the actual values of parameters for which solution of all constraints was numerically obtained; thus, in the first column pressure is not 60, but 60.3 MeV/fm^3. With rising hadronization pressure, the hadronization temperature rises, but it remains well below the phase-transformation temperature. As we have discussed, the low value of T in the chemical-nonequilibrium SHM is consistent with the dynamics of the expansion; the flow of matter reduces the phase-balance T. This, in turn, then requires that the light-quark abundance parameter $\gamma_q \simeq 1.6$. This is the key distinction of the chemical nonequilibrium. It further signals enhancement of the production of baryons over mesons by just this factor. Note that $\gamma_s/\gamma_q \simeq 1.72$. This large ratio means that the yields of Λ and p do not differ much. This indicates strong enhancement of strangeness, a first-day observable of QGP formation, along with ϕ enhancement [23].

VI. COMPARISON OF SHM RESULTS

The large bulk hadronization volume $dV/dy \simeq 4500$ fm^3 suggests that there will be noticeable changes in the Hanbury-Brown–Twiss (HBT) observables, consistent with such a large hadronization volume. The bulk energy content is found in both approaches to be $dE/dy = E/V \times dV/dy = 2.00 \pm 0.05$ TeV per unit of rapidity at $y = 0$. This is the thermal energy of QGP prior to hadronization measured in the local fluid-element rest frame.

The entropy content in the bulk for nonequilibrium, $dS/dy = 13\,860 \pm 64$, is 5% smaller compared to the equilibrium case. This is due to the fact that nonequilibrium particle yields do not maximize entropy. We note that the yields of pions, kaons, and even single strange hyperons are remarkably independent of hadronization pressure or, in the equilibrium case, temperature, even though the volume parameter changes greatly. This effect is counteracted by a balancing change in hadronization temperature, since the yield of charged hadrons is fixed. The hadronization energy density is very close to $E/V \simeq 0.5$ GeV/fm^3, and it tracks the pressure, since the ratio P/E is found to be rather constant.

The yield of multistrange hadrons is much enhanced in the chemical-nonequilibrium model, compared to the equilibrium model, on account of a 50% increased yield of strangeness, which is potentiated for multistrange particles as was predicted to be the signature of QGP [23]. The yield of Λ, for the most favored hadronization condition in both equilibrium and nonequilibrium, can in fact be lower in the nonequilibrium case than in the equilibrium, yet at the LHC the yield of K is always 40% greater. As in the equilibrium results, we observe that several yields are largely independent of the hadronization condition, meaning that ratios such as ϕ/h could be a distinctive signature of hadronization, differentiating the two primary models. This is illustrated in Fig. 1, where the ratio is shown as function of resultant hadronization T.

One can, however, argue that ϕ/h, seen in Fig. 1, could be brought about by strangeness enhancement, not requiring

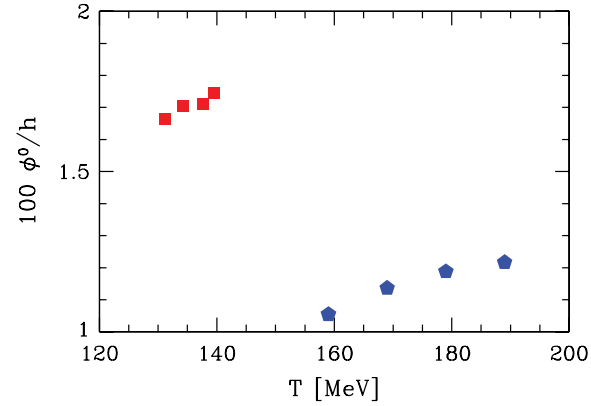

FIG. 1. (Color online) Specific yield ϕ/h for the chemical-equilibrium model (lower right, blue) and the chemical-nonequilibrium model (upper left, red).

that $\gamma_q > 1$; for a more complete discussion, see Ref. [24]. To narrow the choices, we propose to study two more ratios, shown in Fig. 2. The upper frame shows K^*/K^-, as a function of the yield K^-/h. The lower-right (red) nonequilibrium result shows strangeness enhancement at low hadronization T, since K^*/K^- depends mainly on T. We have shown both particle and antiparticle ratios derived from our fixed input for net

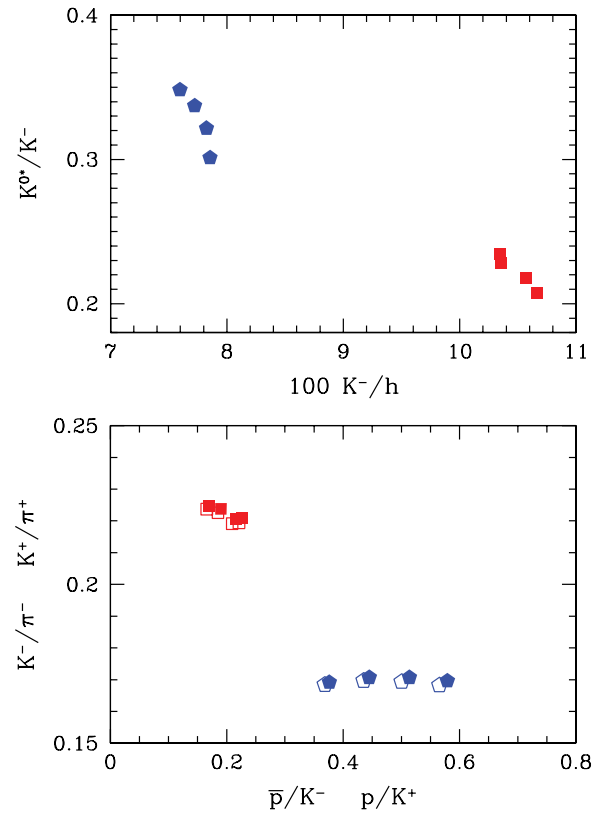

FIG. 2. (Color online) Top frame: Ratio of resonance K^* to kaon yield K, as a function of specific kaon yield K^-/h, for the chemical-equilibrium model (upper left, blue) and the chemical-nonequilibrium model (lower right, red). Bottom frame: K/π ratio, as a function of p/K ratio, for the equilibrium model (lower right, blue) and the nonequilibrium model (upper left, red).

baryon yield to illustrate that differentiation of these results will not be easy.

The bottom frame in Fig. 2 shows the strangeness enhancement in the format of K/π as a function of the most easily measured baryon-to-meson ratio, which is a measure of absolute magnitude of γ—here, specifically $\gamma_q^3/\gamma_s\gamma_q$. We see the equilibrium model at lower right (blue), while the nonequilibrium model is at upper left (red).

VII. SUMMARY AND CONCLUSIONS

We have obtained particle yields within the SHM for the LHC-ion run at $\sqrt{s_{NN}} = 2.76$ TeV. We have discussed both the bulk properties of QGP at breakup and the resulting particle yields. These can vary significantly, depending on the hadronization mechanism. Distinctive features associated with QGP-based strangeness enhancement and final-state chemical nonequilibrium were described, and strategies leading to better understanding of both, the chemical-equilibrium and -nonequilibrium were proposed.

As a function of hadronization conditions, some particle multiplicity lacks diagnostic strength; e.g., kaon yields are seen to be quasiconstant in both models we studied, on account of compensation of T dependence by change in V and other statistical parameters at fixed dh/dy. However, *yields of strange and multistrange particles can vary significantly.* The enhanced yield of strangeness with the phase-space occupancy $\gamma_s \simeq 2.75$ when $\gamma_q \simeq 1.6$ modifies the yield of strange hadrons, and detailed predictions for observables such as ϕ/h, K^*/K, K/π, p/K, and Λ/p were offered. We note that absolute yield of ϕ is enhanced by a factor 1.5 in the nonequilibrium compared to equilibrium hadronization. There is no significant dependence of the ϕ yield on the hadronization condition, making it an ideal first-day observable differentiating chemical equilibrium from nonequilibrium.

The large bulk hadronization volume $dV/dy \simeq 4500$ fm^3 related to HBT observables [25], and the local-rest-frame thermal energy content $dE/dy|_0 = 2$ TeV, constrain hydrodynamic models. A large yield of π^0, η, and thus of associated decay photons is noted, enhanced somewhat in the chemical-nonequilibrium case.

ACKNOWLEDGMENTS

Laboratoire de Physique Théorique et Hautes Energies (LPTHE), at Université Paris 6 and 7, is supported by CNRS as Unité Mixte de Recherche, UMR7589. This work was supported by US Department of Energy Grant No. DE-FG02-04ER41318.

[1] S. Borsanyi *et al.*, J. High Energy Phys. 11 (**2010**) 077.
[2] K. Aamodt *et al.* (ALICE Collaboration), Phys. Rev. Lett. **105**, 252301 (2010).
[3] P. Bozek, M. Chojnacki, W. Florkowski, and B. Tomasik, Phys. Lett. B **694**, 238 (2010).
[4] J. Rafelski and J. Letessier, J. Phys. G **35**, 044042 (2008); Eur. Phys. J. C **45**, 61 (2006).
[5] J. Rafelski and J. Letessier, J. Phys. G **36**, 064017 (2009).
[6] J. Letessier and J. Rafelski, Phys. Rev. C **75**, 014905 (2007).
[7] G. Torrieri, S. Steinke, W. Broniowski, W. Florkowski, J. Letessier, and J. Rafelski, Comput. Phys. Commun. **167**, 229 (2005); G. Torrieri, S. Jeon, J. Letessier, and J. Rafelski, *ibid.* **175**, 635 (2006).
[8] J. Letessier and J. Rafelski, Eur. Phys. J. A **35**, 221 (2008).
[9] F. Becattini and R. Fries, arXiv:0907.1031 [nucl-th].
[10] A. Andronic, P. Braun-Munzinger, and J. Stachel, Nucl. Phys. A **772**, 167 (2006).
[11] A. Andronic, P. Braun-Munzinger, and J. Stachel, Phys. Lett. B **673**, 142 (2009).
[12] F. Becattini, P. Castorina, A. Milov, and H. Satz, Eur. Phys. J. C **66**, 377 (2010).
[13] J. Rafelski, J. Letessier, and G. Torrieri, Phys. Rev. C **72**, 024905 (2005).
[14] A. Andronic *et al.*, Nucl. Phys. A **837**, 65 (2010).
[15] J. Rafelski and J. Letessier, Phys. Rev. Lett. **85**, 4695 (2000).
[16] P. de Forcrand, PoS **LAT2009**, 010 (2009), arXiv:1005.0539 [hep-lat].
[17] G. Endrodi, Z. Fodor, S. D. Katz, and K. K. Szabo, PoS **LAT2008**, 205 (2008), arXiv:0901.3018 [hep-lat]; Z. Fodor and S. D. Katz, arXiv:0908.3341 [hep-ph].
[18] J. Cleymans, J. Phys. G **37**, 094015 (2010).
[19] K. Fukushima, Phys. Lett. B **695**, 387 (2011).
[20] I. Kraus *et al.*, J. Phys. G **32**, S495 (2006); J. Cleymans, I. Kraus, H. Oeschler, K. Redlich, and S. Wheaton, Phys. Rev. C **74**, 034903 (2006).
[21] A. Andronic, P. Braun-Munzinger, and J. Stachel, J. Phys. G **35**, 054001 (2008).
[22] A. T. M. Aerts and J. Rafelski, Phys. Lett. B **148**, 337 (1984).
[23] J. Rafelski, Phys. Rep. **88**, 331 (1982).
[24] M. Petran and J. Rafelski, Phys. Rev. C **82**, 011901(R) (2010); M. Petran, J. Letessier, V. Petracek, and J. Rafelski, Acta Phys. Pol. B **41**, 2785 (2010).
[25] K. Aamodt *et al.* (ALICE Collaboration), Phys. Lett. B **696**, 328 (2011).